FOREX Publication
Open Access | Rapid and quality publishing

International Journal of
Electrical and Electronics Research (IJEER)
Research Article | Volume 11, Issue 4 | Pages 1154-1161 | e-ISSN: 2347-470X

GWOPID-MRAS based Speed Estimation and Speed Control of Sensorless Induction Motors

Saravanan T Y[1] and Dr. Ponnambalam P [2*]
[1]*Research Scholar SELECT, VIT, Vellore, India, saravanan651988@gmail.com*
[2]*Professor, SELECT, VIT, Vellore, India, ponnambalam.p@vit.ac.in*

***Correspondence:** ponnambalam.p@vit.ac.in

ABSTRACT- Sensorless AC motor drives have grown in popularity recently in a variety of applications, from industrial to domestic electrical equipment. FOC and DTC are popular control methodologies in contemporary alternating current (AC) structures. They can achieve good performance for AC motor drives by creating a decupled flux and torque control. However, both have limitations and drawbacks, such as the vector control's dependence on machine parameters and DTC's high flux and torque ripples. This paper proposes a new control method, in which the speed of an induction motor is controlled by Grey Wolf Optimizer (GWO) based PID controller. This method utilizes both FOC, DTC and MRAS observer. The GWOPID controller receives the inputs from MRAS observer, the parameters of PID controller are optimized using GWO algorithm by minimizing the speed deviations of an Induction Motor (IM). The proposed method is implemented in MATLAB/Simulink environment and the performance is compared with IFOC speed control method. Findings demonstrated that the proposed method is effectively reducing the speed deviations as compared with IFOC method under different load conditions

Keywords: Direct Torque Control (DTC), Grey Wolf Optimizer (GWO).

ARTICLE INFORMATION
Author(s): Saravanan T Y and Dr. Ponnambalam P;
Received: 18/08/2023; **Accepted**: 20/10/2023; **Published**: 20/12/2023;
e-ISSN: 2347-470X;
Paper Id: IJEER 1808-08;
Citation: 10.37391/IJEER.110436
Webpage-link:
https://ijeer.forexjournal.co.in/archive/volume-11/ijeer-110436.html

Publisher's Note: FOREX Publication stays neutral with regard to Jurisdictional claims in Published maps and institutional affiliations.

1. INTRODUCTION

Because of their endurance and low maintenance needs, IMs are increasingly swapping conventional DC motors in engineering applications. Even though the affordable, low-performance volt/frequency (V/f) control method is often adequate, some applications that demand high dynamic performances, including servo motors and EVs, require the vector control technique. In conventional high performance indirect vector control, speed or position measurements are often made via an encoder or tachometer. Unfortunately, because it is sensitive to mechanical vibrations and dust, a sensor of this type is not suited for tough situations. Furthermore, mounting this kind of sensor on the motor shaft might occasionally be challenging. Sensorless regulation of (IM) has thus been a tough study issue in the last ten years, according to [11]-[3]. The various approaches anticipated in the prose can be viewed as attempts to improve flux and speed estimation by providing some input to voltage integration rather than none [4]. A rapidly growing area in recent years. We recently suggested [12] a strategy for lowering input power and enhancing IM drive efficiency called golden-section search. In the second phase of the inquiry, we employ sensorless control approaches.

AC drive high-performance control necessitates torque and flux control are decoupled. It accomplished using two methodologies, FOC and DTC. The vector control aims to provide the same behavior as a separate excitation DC motor, Furthermore, the FOC method necessitates the axis coordinate transformation, which adds to its complexity [13]. In contrast to vector control, Direct Torque features a simpler control system, faster reaction, and less parameter dependence. Furthermore, it is not subject to current regulations. It uses a switching and hysteresis flux and torque controller to select the inverter voltage vector. After all, due to its construction, DTC suffers from ripples and switching frequency, which can cause acoustical noise, reduce the performance of the controlled machine, and present control challenges in low-speed zones [14-15]. In this paper a hybrid control technique is proposed, that combines two different methods and simplifies their complexities in order to improve the performance of FOC and DTC and gain the main advantages of both of them as: a decoupled control and simple implementation with reducer ripples level and low parameters depend. This control approach is based on CVC in conjunction with a DTC switching table. Another goal of this research is to replace the mechanical sensor with a sensorless algorithm in order to reduce system costs and increase dependability [16]. The observers continue to be an important subject of study in this science. Several significant studies, sliding mode observers [18], extended Kalman filter [17], and adaptive Luenberger observers [18] have been presented. Because of its simplicity, the model reference adaptive systems (MRAS) method is extensively employed. Numerous MRAS structures, such as rotor flux, reactive power, and reverse EMF, have been characterized in the literature [19-21]. Schauder's [22] rotor flux MRAS approach is the most extensively used MRAS strategy. This study describes a hybrid

FOREX Publication
Open Access | Rapid and quality publishing
International Journal of Electrical and Electronics Research (IJEER)
Research Article | Volume 11, Issue 4 | Pages 1154-1161 | e-ISSN: 2347-470X

FOC-DTC control approach for induction motor driving using a speed MRAS observer for speed reconstruction.

2. DIFFERENT COLOR METHODS

2.1 Field Oriented Control

The main basis of the FOC technique is to regulate the induction motor drive to provide greater dynamic response and torque and flux control decoupling [13,16]. The IM torque expression with flux in d-q frame is as follows:

$$T_e = \frac{P}{2}\frac{M_{sr}}{L_r}\left(\varphi_{dr} i_{qs} - \varphi_{qr} i_{ds}\right) \quad (1)$$

From the field-oriented model

$$\psi_{rd} = \psi_r; \qquad \psi_{rq} = 0 \quad (2)$$

The electromagnetic torque and rotor flux can be expressed as follows:

$$T_e = \frac{P}{2}\frac{M}{L_r}\left(\varphi_{dr} i_{qs}\right) \quad (3)$$

$$\varphi_r = \varphi_{dr} = M i_{ds} \quad (4)$$

$$\omega_{slip} = \frac{R_s i_{qs}^*}{L_r i_{ds}^*} \quad (5)$$

A simple PI regulator controls the majority of the speed [3–4]. A decoupled GWOPI controller and PWM modulator acting as a voltage controller can control or three phase hysteresis comparators as a current IFOC controller. The hysteresis control uses hysteresis bands to compare the reference currents with the measured values in order to produce the VSI switching states.

2.2 Direct Torque Control

Using an induction motor model, the Direct Torque Control method estimates the voltage necessary to produce a given output torque. Using only current and voltage measurements, it is possible to estimate the instantaneous stator flux and output torque [15].

Table 1: Switching Table

Sector/ Error		I	II	III	IV	V	VI
dΨs=1	dTe=1	V2	V3	V4	V5	V6	V1
	dTe=0	V7	V0	V7	V0	V7	V0
	dTe=-1	V6	V1	V2	V3	V4	V5
dΨs=0	dTe=1	V3	V4	V5	V6	V1	V2
	dTe=0	V0	V7	V0	V7	V0	V7
	dTe=-1	V5	V6	V1	V2	V3	V4

$$T_e = \frac{PM}{2\alpha L_s L_r}|\varphi_s||\varphi_r| sin\delta \quad (6)$$

The torque and flux are controlled by two comparators. Table. I calculate the voltage vector.

Based on FOC theory [20-21]:

$$\begin{cases} |\psi_r| = K_d i_{ds} \\ T_e = K_q i_{qs} \end{cases} \Rightarrow \begin{cases} |\psi_r| \alpha i_{ds} \\ T_e \alpha i_{qs} \end{cases} \Rightarrow \begin{cases} \Delta|\psi_r| \alpha \Delta i_{ds} \\ \Delta T_e \alpha \Delta i_{qs} \end{cases} \quad (7)$$

2.3 MRAS Speed Observer Design

This method is a combination of voltage model and current model based on voltage and currents [22], [25-26]. The current and voltage models are also known as reference model and adaptive models, and presented in *equation (8) and (9).*

$$\begin{cases} \dot{\psi}_{r\alpha} = \frac{L_r}{M_{sr}}\left(V_{s\alpha} - R_s i_{s\alpha} - \sigma L_s i_{s\alpha}\right) \\ \dot{\psi}_{r\beta} = \frac{L_r}{M_{sr}}\left(V_{s\beta} - R_s i_{s\beta} - \sigma L_s i_{s\beta}\right) \end{cases} \quad (8)$$

$$\begin{cases} \hat{\dot{\psi}}_{r\alpha} = \frac{M_{sr}}{T_r} i_{s\alpha} - \frac{1}{T_r}\hat{\psi}_{r\alpha} - \hat{\omega}\hat{\psi}_{r\beta} \\ \hat{\dot{\psi}}_{r\beta} = \frac{M_{sr}}{T_r} i_{s\beta} - \frac{1}{T_r}\hat{\psi}_{r\beta} - \hat{\omega}\hat{\psi}_{r\alpha} \end{cases} \quad (9)$$

$$\hat{\omega} = \left(K_p + \frac{K_i}{s}\right) e_{\psi_r} \quad (10)$$

The general MRAS observer diagram is shown in *figure 1* [23], [26].

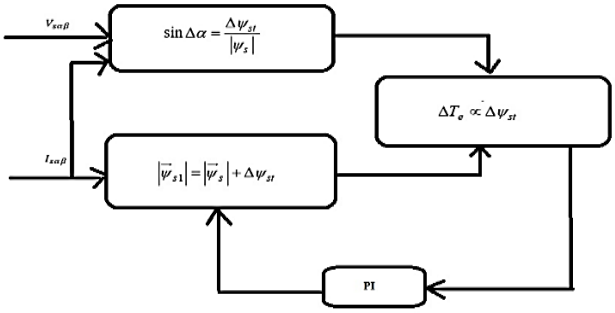

Figure 1: Diagram of MRAS speed observer

3. GREY WOLF OPTIMIZER BASED PID CONTROLLER DESIGN

It was proposed by Seyedali Mirjalili, Seyed Mohammad Mirjalili, and Andrew Lewis in 2014 as a way to solve optimization problems. GWO is a type of swarm intelligence algorithm that is utilized in a variety of sectors to solve challenging optimization problems.

Initialization: The process begins by populating a population of "wolves," with each wolf representing a possible solution to the optimization problem. The population size is set by the user.

Objective Function: The optimization problem involves an objective function that needs to be minimized or maximized. This function evaluates the quality of a solution (wolf) in the problem space.

Hierarchy and Hunting Behavior: In the context of optimization, this behavior is translated into the concept of hierarchy among the wolves based on their fitness values. The wolves are categorized into four different roles based on their fitness:
Alpha Wolf, Beta Wolf, Delta Wolf and Omega Wolf.

FOREX Publication
Open Access | Rapid and quality publishing
International Journal of Electrical and Electronics Research (IJEER)
Research Article | Volume 11, Issue 4 | Pages 1154-1161 | e-ISSN: 2347-470X

Updating Positions: To explore and utilize the search space, the wolves' placements are updated after each iteration. In order to do this, the positions of the alpha, beta, and delta wolves are used to update each wolf's position. The new position of a wolf is calculated using mathematical formulas that take into account the positions of other wolves and some control parameters.

Exploration and Exploitation: The GWO algorithm balances exploration and. The movement of wolves towards the alpha, beta, and delta wolves encourages exploitation, while the randomization factor encourages exploration.

Termination: The algorithm continues to update the positions of wolves for a certain number of iterations or until a stopping criterion is met.

Solution Extraction: The solution that corresponds to the alpha wolf (best fitness) at the end of the optimization process is considered the final optimized solution to the problem.

Implementation of GWO:
The structure of GWO based conventional PID controller is shown in *figure 4.2*. The controllable parameters are K_p, K_i and K_d, these parameters are obtained using GWO algorithm.

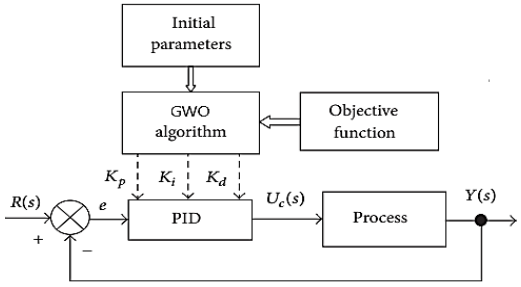

Figure 2: Structure of GWOPID

Figure 2 depicts the general hybrid FOC-DTC strategy control method.

The procedures adopted for obtaining controllable parameters are K_p, K_i and $K_d$is shown in *figure 3*.

Step 1: Generate initial positions of X_i^0, initialize the values of a, A & C, Load test system data.

Generate initial positions of X_i^0 for $i = 1,2,3 \dots \dots n$. Initialize the values of a, A & C, maximum number of iterations (K_{max}).

Step 2: Assume initial conditions that are required for simulation of Induction motor.

Run the simulation file of three phase induction motor with test system data and calculate Integral Time Area Error (ITAE) of speed

Step 3: Calculation of fitness function of each search agent and select three best search agents.
Calculate the fitness function using the *equation (11)* for all the search agents and select three best search agents $(X_\alpha, X_\beta \& X_\delta)$ which are giving best fitness values.

$$J = \frac{1}{ITAE} \quad (11)$$

Step 4: Update the position of current search agent.

Update the position of current search agent by using the *equations (12) to (20).*

$$\vec{D}_\alpha = \left|\vec{C}_1 * \vec{X}_\alpha - \vec{X}\right| \quad (12)$$
$$\vec{D}_\beta = \left|\vec{C}_2 * \vec{X}_\beta - \vec{X}\right| \quad (13)$$
$$\vec{D}_\delta = \left|\vec{C}_3 * \vec{X}_\delta - \vec{X}\right| \quad (14)$$
$$\vec{X}_1 = \vec{X}_\alpha - \vec{A}_1 * \vec{D}_\alpha \quad (15)$$
$$\vec{X}_2 = \vec{X}_\beta - \vec{A}_2 * \vec{D}_\beta \quad (16)$$
$$\vec{X}_3 = \vec{X}_\delta - \vec{A}_3 * \vec{D}_\delta \quad (17)$$

Where, the vectors $\vec{A}_1, \vec{A}_2, \vec{A}_3$and $\vec{C}_1, \vec{C}_2, \vec{C}_3$are calculated using the *equations (18) and (19)* with different random values of $\overrightarrow{rv}_1$ and $\overrightarrow{rv}_2$. The parameter $\vec{a}$ is initially taken as 2 and moves towards 0.

$$\vec{A} = 2 * \vec{a} * \overrightarrow{rv}_1 - \vec{a} \quad (18)$$
$$\vec{C} = 2 * \overrightarrow{rv}_2 \quad (19)$$

The current search agent position is written as:

$$\vec{X}_{(k+1)} = \frac{\vec{X}_1 + \vec{X}_2 + \vec{X}_3}{3} \quad (20)$$

Step 5: Update the vectors a, A & C.

Using the *equations (19), (20) and (21)*, update the vectors a, A & C.

$$\vec{a} = 2 - \frac{k}{k_{max}} \quad (21)$$

Step 6: fitness function calculation.

Calculate the fitness function using the *equation (11)* for all search agents.

Step 7: Update the positions of $X_\alpha, X_\beta \& X_\delta$.

After the fitness function calculation, then update the positions of $X_\alpha, X_\beta \& X_\delta$ using the following steps:

$If\ (fitness < \alpha_{Score})$
$\alpha_{Score} = fitness;$
$Update\ \alpha\ position\ using\ the\ equation\ (12)$
$else$
$If\ (fitness > \alpha_{Score} \&\& fitness < \beta_{Score})$
$\beta_{Score} = fitness;$
$Update\ \beta\ position\ using\ the\ equation\ (13)$
end
$else$
$If\ (fitness > \alpha_{Score} \&\& fitness > \beta_{Score} \&\& fitness < \delta_{Score})$
$\delta_{Score} = fitness;$
$Update\ \delta\ position\ using\ the\ equation\ (14)$
end
end

FOREX Publication
Open Access | Rapid and quality publishing
International Journal of Electrical and Electronics Research (IJEER)
Research Article | Volume 11, Issue 4 | Pages 1154-1161 | e-ISSN: 2347-470X

Step 8: Check the fitness function condition and iteration condition.

Check the fitness function is satisfied or not using *the equation (22)* and check iterations equal to the maximum number of iterations using the *equation (23)*. If these two conditions are satisfying, then stop the procedure and return speed. Otherwise, increase iteration by one and then repeat steps from 2 to 8.

$$J^K - J^{K-1} < \varepsilon \quad (22)$$

$$K \geq K_{max} \quad (23)$$

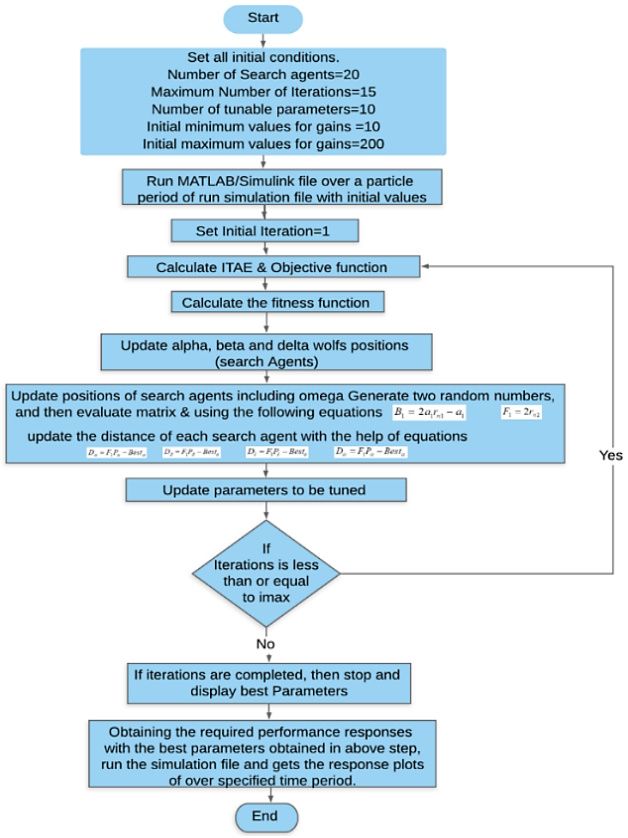

Figure 3: GWO flowchart for PID controller

4. SIMULATION RESULT

The simulation diagram is shown in *figure 4* and the respective results are shown in the *figures 5 to 24*.

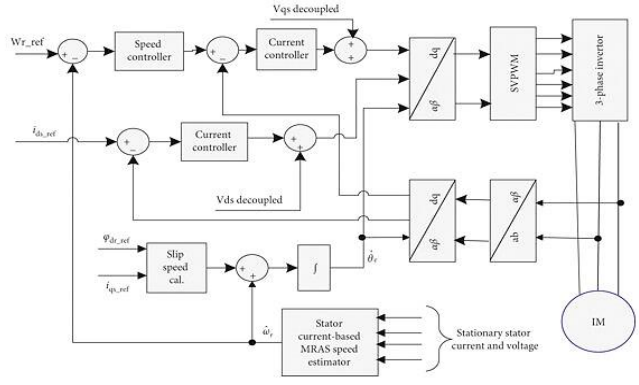

Figure 4: GWO-PI-MRAS method representation

The proposed approach is evaluated under various speed situations with varying load torques.

Case A: 2000 rpm speed is given as reference speed, shown in *figure 6*. Load torque is taken as a variable, it varies in three stages during the simulation time period and is shown in *figure 5*. From *figure 6*, the load torque is initially 0 during 0-0.5 seconds; later increased to 792 Nm up to 1.5 seconds; then decreased to -792 Nm.

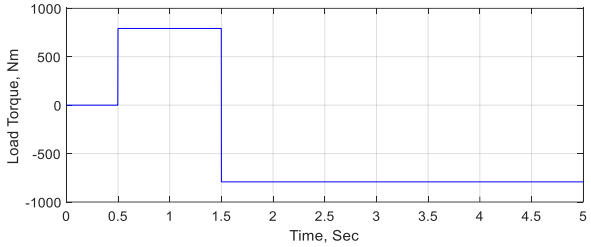

Figure 5: Induction motor load torque with respect to time

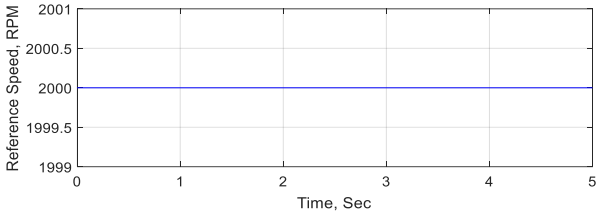

Figure 6: Typical Speed characteristic of Induction motor

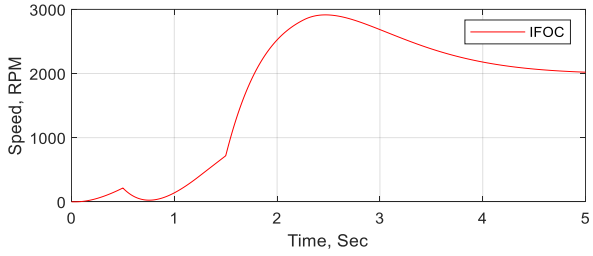

Figure 7: IFOC controller-controlled IM speed response

Figure 7 depicts IFOC controller-controlled IM speed response. It takes 4.5 seconds using an IFOC controller to achieve the speed after max overrun up to 2940 rpm. From this figure, it is clear that initially speed increases and then decreases during 0-1 second after that reaching to 2940 at 2.4 seconds and then decreased to 2000 after 4.5 seconds.

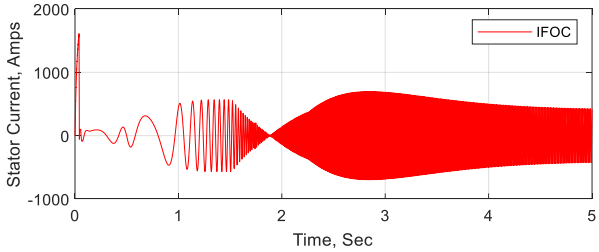

Figure 8: Response of the IM's stator current to the IFOC controller

Figure 8 depicts the stator current with IFOC. After 4.5 seconds, the stator current is steady. This figure shows that, the stator current controlled by IFOC is increasing and decreasing

FOREX Publication
Open Access | Rapid and quality publishing
International Journal of Electrical and Electronics Research (IJEER)
Research Article | Volume 11, Issue 4 | Pages 1154-1161 | e-ISSN: 2347-470X

during the interval 0-4.5 seconds after 4.5 seconds the stator current is consistent.

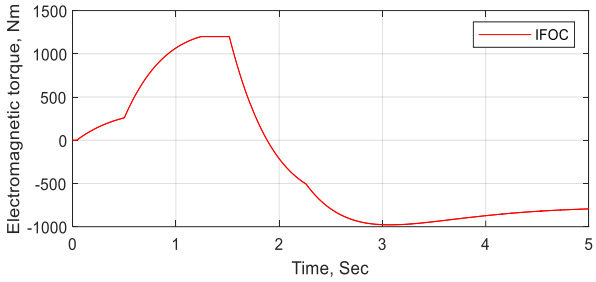

Figure 9: Response of the IM's magnetic torque to the IFOC controller

Figures 9 demonstrate Response of the IM's magnetic torque to the IFOC controller. This figure indicates that torque increased up to 1.8 seconds and then decreased exponentially up to 2.9 seconds after slowly increased and maintain steady value from 4.5 seconds onwards.

Figures 10 demonstrate DC Bus voltage with IFOC controller. This figure indicates that voltage increased and then decreased up to 2.0 seconds after increased up to 2.9 seconds and then decreased uo to 4.5 seconds after that maintain steady value from 4.5 seconds onwards.

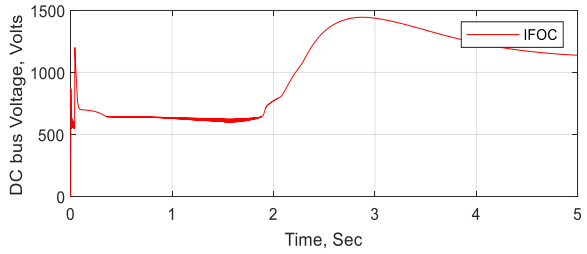

Figure 10: DC Bus voltage with IFOC controller

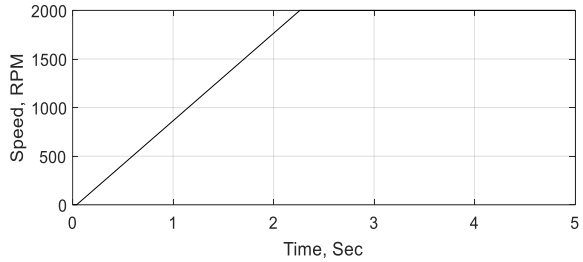

Figure 11: GWO-PID-MRAS controller speed responsiveness of IM

GWO-PID-MRAS controller speed responsiveness of IM is shown in *figure 11*. With this controller speed is linearly increasing up to 2.3 seconds and then maintains constant speed of 2000. No overrun is identified with this controller, which reduces the overrun by 31.97% and 48.89% reduction in settling time period.

Stator Response of the IM's stator current to the GWO-PID-MRAS controller is shown in *figure 12*. Stator current varies proportionately with respect to torque variations without heavy overshoot.

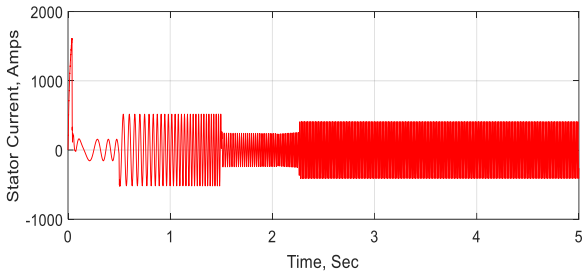

Figure 12: Stator Response of the IM's stator current to the GWO-PID-MRAS controller

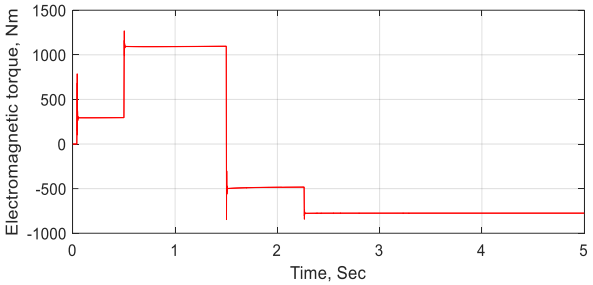

Figure 13: IM's magnetic torque when controlled by a GWO-PID-MRAS system

IM's magnetic torque when controlled by a GWO-PID-MRAS system is shown in *figure 13*. Initially the EM increased and then settled up to 0.5 seconds, after 0.5 seconds suddenly increased to 1100 and then mains constant up to 1.5 seconds; after 1.5 seconds suddenly decreased to -500 and maintained up to 2.3 seconds; after 2.3 seconds it maintained -792 consistently.

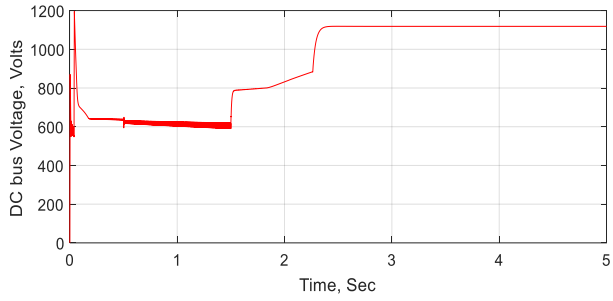

Figure 14: DC bus voltage with GWO-PID-MRAS controller

Figures 14 demonstrate DC bus voltage with GWO-PID-MRAS controller. The proposed controller decreases the voltage oscillations of the bus within 2.5 seconds after that it maintains a constant voltage of 1100.

Case B: Speed is taken as variable; it varies in two stages during simulation is shown in *figure 17*. from *figure 17*, 2000 rpm speed is given as reference speed during 0-5 seconds and 3000 rpm during 5-10 rpm. Load torque is taken as a variable, it varies in three stages during the simulation time period and is shown in *figure 5*. From *figure 16*, the load torque is initially 0 during 0-3 seconds; later increased to 792 Nm up to 6 seconds; then decreased to -792 Nm.

FOREX Publication
Open Access | Rapid and quality publishing
International Journal of Electrical and Electronics Research (IJEER)
Research Article | Volume 11, Issue 4 | Pages 1154-1161 | e-ISSN: 2347-470X

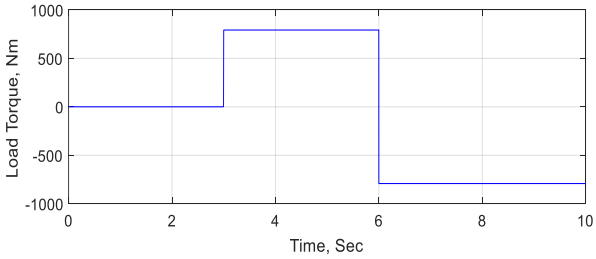

Figure 15: Load torque

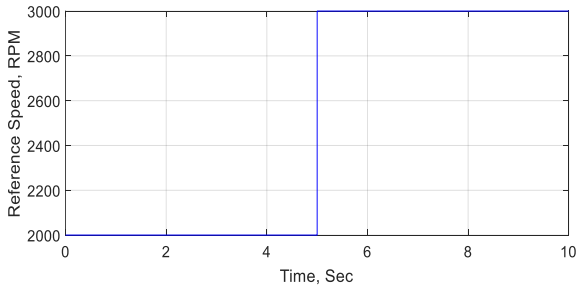

Figure 16: Reference Speed

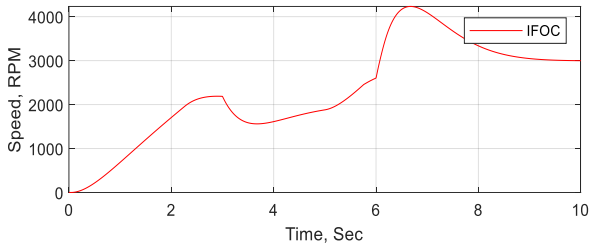

Figure 17: IFOC controller-controlled IM speed response

Figure 17 depicts the speed of an IM using an IFOC controller. To reach reference speeds of 2000 and 3000 rpm it takes 4.5 seconds and 8.2 seconds respectively with overshoots of 2400 and 4050 rpms.

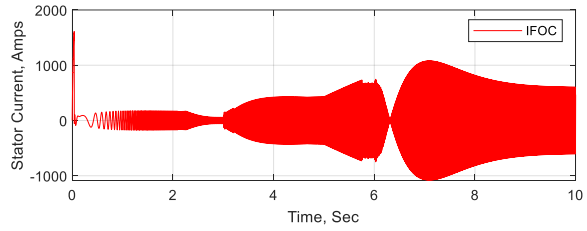

Figure 18: Response of the IM's stator current to the IFOC controller

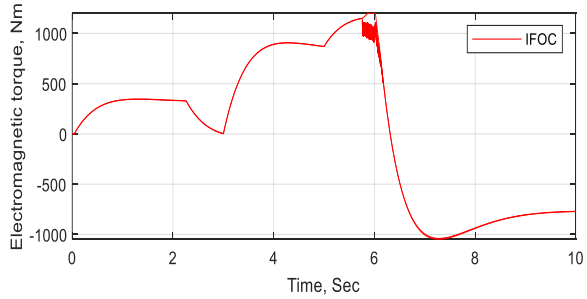

Figure 19: Response of the IM's magnetic torque to the IFOC controller

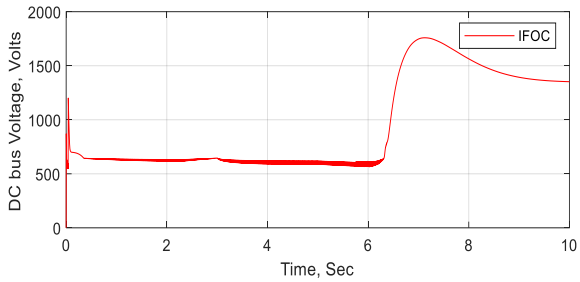

Figure 20: DC Bus voltage with IFOC controller

Figures 18 to 20 depict the responses of the stator current, electromagnetic torque, and DC bus voltage.

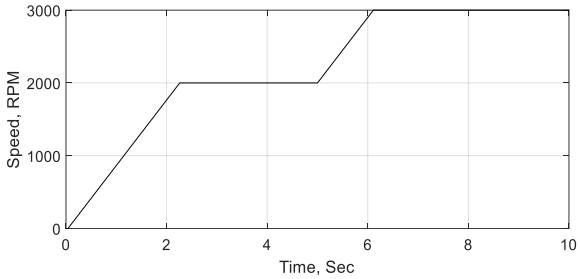

Figure 21: Speed response of IM with GWO-PID-MRAS controller

Figure 21 depicts the speed of an IM with a GWO-PID-MRAS controller. To reach reference speeds of 2000 and 3000 rpm it takes 2.3 seconds and 6 seconds respectively with overshoots of 2000 and 3000 rpms.

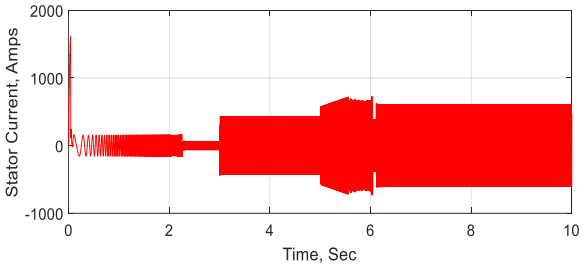

Figure 22: Stator current response of IM with GWO-PID-MRAS controller

Stator Response of the IM's stator current to the GWO-PID-MRAS controller is shown in *figure 22*. Stator current varies proportionately with respect to torque variations without heavy overshoot.

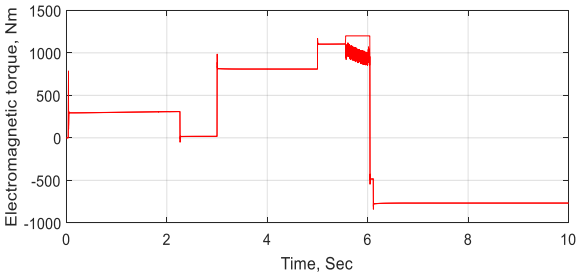

Figure 23: Electromagnetic torque of IM with GWO-PID-MRAS controller

FOREX Publication
Open Access | Rapid and quality publishing
International Journal of Electrical and Electronics Research (IJEER)
Research Article | Volume 11, Issue 4 | Pages 1154-1161 | e-ISSN: 2347-470X

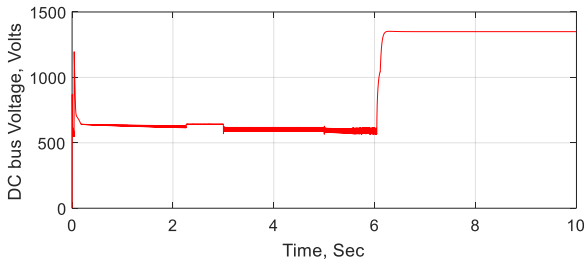

Figure 24: DC bus voltage with GWO-PID-MRAS controller

Table 2: Speed variations with IFOC Controller under different load torque conditions

Speed variations with IFOC Controller under different load torque conditions		
Case:A (Reference speed: 2000 rpm)	Peak (rpm)	2940
	Settling Time (sec)	4.5
Case:B (Reference speed: 2000 rpm)	Peak (rpm)	2400
	Settling Time (sec)	4.5
Case:B (Reference speed: 3000 rpm)	Peak (rpm)	4050
	Settling Time (sec)	8.2

Table 3: Speed variations with GWO-PID-MRAS Controller under different load torque conditions

Speed variations with GWO-PID-MRAS Controller under different load torque conditions		
Case:A (Reference speed: 2000 rpm)	Peak (rpm)	2000
	Settling Time (sec)	2.3
Case:B (Reference speed: 2000 rpm)	Peak (rpm)	2000
	Settling Time (sec)	2.3
Case:B (Reference speed: 3000 rpm)	Peak (rpm)	3000
	Settling Time (sec)	6

IM's magnetic torque when controlled by a GWO-PID-MRAS system is shown in *figure 23*. Initially the EM increased and then settled up to 2.2 seconds, after 2.2 seconds suddenly decreased to 0 and then mains constant up to 5 seconds; after 5 seconds suddenly increased to 1100 and maintained up to 26 seconds; after 6 seconds suddenly decreased and it maintained -792 consistently.

Figure 14 demonstrate DC bus voltage with GWO-PID-MRAS controller. The proposed controller decreases the voltage oscillations of the bus within 6 seconds after that it maintains a constant voltage of 1300.

From these results, it is clear that the proposed method performance is better as compared with IFOC controller irrespective of Load torques and Speeds.

5. CONCLUSION

A novel speed estimation and control method for sensorless induction motors was proposed in this research. This method combines FOC and DTC speed control methods, and a MRAS observer is utilized to estimate speed. PID controller parameters are optimized using the GWO algorithm with the decrease of speed deviations as the objective function. The proposed approach was implemented in MATLAB/Simulink and the results were compared to the IFOC method under various loading circumstances. The results show that, regardless of loading conditions, the suggested method efficiently reduces speed deviations when compared to the IFOC method.

Nomenclature

P	: No. of poles
φ_{dr}	: Direct axis stator flux
φ_{qr}	: Quadrature axis stator flux
i_{ds}	: Direct axis stator current
i_{qs}	: Quadrature axis stator current
M	: Mutual inductance between stator & rotor
L_r	: Rotor inductance
L_s	: Stator inductance
ω_{slip}	: Slip frequency
R_r	: Rotor resistance
α	: Blondel's coefficient
δ	: Angle between stator and rotor

REFERENCES

[1] K. Rajashekara, A. Kawamura, K. Matsuse (editors), Sensorless Control of AC Motor Drives, IEEE Press, New York, 1996.

[2] P. Vas, Sensorless Vector and Direct Torque Control,Oxford University Press, Oxford, 1998.

[3] I. Holtz, "Sensorless Position Control of Induction Motors -An Emerging Technology ", IEEE Trans.on Industrial Electronics, Vol. 45, No. 6,

[4] K.D. Hurst, T.G. Hahetler, G. Griva, F. Profumo, '2ero-speed tacholess IM torque control: simply a matter of stator voltage integration," IEEE Transactions on Industry Applications, Vol. 34, No. 4, July-Aug. 1998, pp. 790 -795.

[5] Y.P. Landau, Adaptive Control: Thc Model Reference Approach, Marcel Dekker, New York, 1979.

[6] S.Tamai, H. Sugimoto, M. Yano, "Speed sensor-less vector control of induction motor with model reference adaptive system," Coni Record of the 1985 IEEE-IAS Annual Meeting, pp. 613-620.

[7] C. Schauder, "Adaptive speed identification for vector control of induction motors without rotational transducers," IEEE Trans. Ind. Applicat., vol. 28, no. 5 , Sep./Oct. 1992,pp. 1054-1061.

[8] H. Tajima, Y. Hori, "Speed sensorless field-orientation control of the induction machine," IEEE Trans.h d . Applicat., vol. 29, no. I , Jan./Feb.1993, pp. 175-180.

[9] F.Z. Peng, T. Fukao, ''Robust speed identification for speed-sensorless vector control of induction motors,'' IEEE Trans. Ind. Applicat., vol. 30, no. 5, pp. 1234-1240, Sep./Oct. 1994.

[10] F.Z. Peng, T. Fukao, J.S. Lai, "Low-speed performance of robust speed identification using instantaneous reactive power for tacholess vector control of induction motors," Conference Record of the 1994 IEEE-IAS Annual Meeting, Vol. 1, pp. 509 -5 14.

[11] Y. Hori, T. Umeno, "Implementation of robust fluxobserver based field orientation (FOFO) controller for induction machines," IEEE-IAS Conz Rec.,pp. 523-528, 1989.

[12] M. Ta-Cao, Y. Hori, "Convergence improvement of eficiency-optimization control of induction motor drives," Coni Record of the 35st IEEE-IAS Annuol Meeting, Rome, Italy, Oct. 2000, Vol. 3, pp. 1662-1669.

[13] D. Casadei, F. Profumo and A. Tani, "FOC and DTC:two viable schemes for induction motors torque control", IEEE Transactions on Power Electronics, vol. 17,no. 5, pp. 779-787, 2002.

[14] M. Farasat, A. Trzynadlowski and M. Fadali, "Efficiency improved sensorless control scheme for electric vehicle induction motors", IET Electrical Systems in Transportation, vol. 4, no. 4, pp. 122-131, 2014.

[15] Y. Ren and Z. Zhu, "Reduction of Both Harmonic Current and Torque Ripple for Dual Three-Phase Permanent-Magnet Synchronous Machine

International Journal of
Electrical and Electronics Research (IJEER)
Research Article | Volume 11, Issue 4 | Pages 1154-1161 | e-ISSN: 2347-470X

Using Modified Switching-Table-Based Direct Torque Control", IEEE Trans. Ind. Electron., vol. 62, no. 11, pp. 6671-6683, 2015.

[16] D. Holmes, B. McGrath and S. Parker, "Current Regulation Strategies for Vector-Controlled Induction Motor Drives", IEEE Trans. Ind. Electron., vol. 59, no. 10, pp. 3680-3689, 2012.

[17] X. Fu and S. Li, "A Novel Neural Network Vector Control Technique for Induction Motor Drive", IEEE Transactions on Energy Conversion, vol. 30, no. 4, pp. 1428-1437, 2015.

[18] A. Ammar, A. Bourek and A. Benakcha, "Modified load angle Direct Torque Control for sensorless induction motor using sliding mode flux observer", in 2015 4th International Conference on Electrical Engineering (ICEE), Boumerdes, Algeria, 2015.

[19] B. Singh, S. Dwivedi, S. Jain, Torque ripple reduction technique with improved flux response for a direct torque control induction motor drive, IET Power Electronics. 6 (2013) 326-342.

[20] S. Vaez-Zadeh and E. Jalali, "Combined vector control and direct torque control method for high performance induction motor drives", Energy Conversion and Management, vol. 48, no. 12, pp. 3095-3101, 2007.

[21] H. Karimi, S. Vaez-Zadeh and F. Rajaei Salmasi, "Combined Vector and Direct Thrust Control of Linear Induction Motors with End Effect Compensation", IEEE Transactions on Energy Conversion, vol. 31, no. 1, pp. 196-205, 2016.

[22] S. Gadoue, D. Giaouris and J. Finch, "MRAS Sensorless Vector Control of an Induction Motor Using New SlidingMode and Fuzzy-Logic Adaptation Mechanisms", IEEE Transactions on Energy Conversion, vol. 25, no. 2, pp. 394-402, 2010.

[23] I. Benlaloui, S. Drid, L. Chrifi-Alaoui and M. Ouriagli, "Implementation of a New MRAS Speed Sensorless Vector Control of Induction Machine", IEEE Transactions on Energy Conversion, vol. 30, no. 2, pp. 588-595, 2015.

[24] A. Smith, S. Gadoue and J. Finch, "Improved Rotor Flux Estimation at Low Speeds for Torque MRAS-Based Sensorless Induction Motor Drives", IEEE Transactions on Energy Conversion, vol. 31, no. 1, pp. 270-282, 2016.

[25] C. Schauder, "Adaptive speed identification for vector control of induction motors without rotational transducers", IEEE Transactions on Industry Applications, vol. 28, no. 5, pp. 1054-1061, 1992.

[26] H. Tajima and Y. Hori, "Speed sensorless fieldorientation control of the induction machine", IEEE Transactions on Industry Applications, vol. 29, no. 1, pp.175-180, 1993.

[27] F. Alonge, F. D'Ippolito and A. Sferlazza, "Sensorless Control of Induction-Motor Drive Based on Robust Kalman Filter and Adaptive Speed Estimation", IEEE Trans. Ind.Electron., vol. 61, no. 3, pp. 1444-1453, 2014.